Resilient Cities and Structures 1 (2022) 24–39

Contents lists available at ScienceDirect

Resilient Cities and Structures

journal homepage: www.elsevier.com/locate/rcns

Full Length Article

On the effects of salient parameters for an efficient probabilistic seismic loss assessment of tunnels in alluvial soils

Zhongkai Huang[a,*], Kyriazis Pitilakis[b,*], Dongmei Zhang[a], Grigorios Tsinidis[c], Sotirios Argyroudis[d]

[a] Key Laboratory of Geotechnical and Underground Engineering of Ministry of Education, Department of Geotechnical Engineering, Tongji University, Shanghai 200092, China
[b] Department of Civil Engineering, Aristotle University of Thessaloniki, Thessaloniki, Greece
[c] Department of Civil Engineering, University of Thessaly, Volos, Greece
[d] Department of Civil and Environmental Engineering, Brunel University London, London, United Kingdom

ARTICLE INFO

Keywords:
Seismic risk
Loss assessment
Metro tunnels
Fragility functions
Infrastructure resilience

ABSTRACT

Tunnels are critical infrastructure for the sustainable development of urban areas worldwide, especially for modern metropolises. This study investigates the effects of salient parameters, such as the soil conditions, tunnel burial depth, tunnel construction quality, and aging phenomena of the lining, on the direct seismic losses of circular tunnels in alluvial deposits when exposed to ground seismic shaking. For this purpose, a practical approach is employed to probabilistically assess the direct losses of single tunnel segment with unit length, as well as of tunnel elements representative of the Shanghai Metro Lines 1 and 10, assuming various levels of seismic intensity. The findings of this study can serve as the basis for decision-making, seismic loss, and risk management based on the principles of infrastructure resilience.

1. Introduction

Tunnels play a critical role in a national infrastructure system, which is vulnerable to seismic hazards, often with negative implications such as emergency response impairment, potential casualties [1–2], societal and economic losses [3–5]. The collapse of the Daikai subway station during the 1995 Kobe earthquake in Japan [6,7] and the collapse of mountain tunnels during the 2008 Wenchuan earthquake in China [8,9] constitute typical examples. Since the 1990s, the seismic safety of tunnels has become an essential consideration in seismic-prone areas. Moreover, the earthquake-induced tunnel damage may affect regular traffic operations and people's life safety. Even minor or moderate damage of tunnels caused by seismic hazards may require significant time and cost of repair, ultimately posing an overall adverse impact on the societies and the economy [10]. From this perspective, understanding the vulnerability of critical infrastructure and characterizing its resilience is essential [11–13], toward making cities more resilient to extreme events such as earthquakes [14]. Thus, it is essential to quantify the seismic fragility of tunnels and assess the loss of underground systems, which can inform priorities for mitigation measures to enhance city resilience.

In recent decades, scholars worldwide focused on seismic vulnerability assessment of tunnels by providing fragility functions for such assessment based on empirical, analytical, and numerical approaches. The fragility functions (i.e., curves, surfaces) can be used to evaluate tunnel vulnerability under different seismic scenarios and serve as the basis for the seismic loss analysis of tunnels. ALA [15] developed a series of empirical fragility curves based on the earthquake-induced damage cases, reported during past earthquakes. Balkaya and Kalkan [16] investigated the seismic fragility of a tunnel, and corresponding strengthening measures were proposed. Argyroudis and Pitilakis [17] developed a set of analytical fragility curves for typical circular and cut and cover tunnels buried in different soil conditions, accounting for the randomness of ground seismic shaking. Since then, many studies have focused on the development of analytical fragility functions for the assessment of tunnels and underground structures (e.g., subway stations), accounting for salient parameters, e.g., tunnel/structure typologies [18,19], tunnel/structure buried depths [20–22], construction quality and aging effects [23,24], as well as the effect of the vertical component of ground shaking [25]. More recently, He et al. [26] examined the seismic fragility of a typical underground structure, considering the effect of spatially varying soil properties. More information about recent advances in the seismic fragility analysis of tunnels and other underground structures may be found in Tsinidis et al. [27].

Numerous loss assessment frameworks have been proposed and applied for buildings [28,29], bridges [30,31], and other critical infrastructure [32–35]. However, few studies focused on the probabilistic seismic

* Corresponding authors.
E-mail addresses: 5huangzhongkai@tongji.edu.cn (Z. Huang), kpitilak@civil.auth.gr (K. Pitilakis).

https://doi.org/10.1016/j.rcns.2022.10.006
Received 1 September 2022; Received in revised form 19 October 2022; Accepted 20 October 2022

loss analysis of tunnels [36,37]. Selva et al. [36] discussed the effects of inter-model variability of fragility curves on the seismic loss and risk assessment of tunnels. Cartes et al. [37] presented a framework for the selection of fragility curves for the seismic risk assessment of tunnels in Chile. To the best of the author's knowledge, the effects of salient parameters, such as soil conditions, tunnel buried depths, tunnel construction quality, or aging phenomena of the lining, have not been considered so far in the literature in the seismic loss assessment of tunnels, thus this is an important step forward for an efficient and well-informed loss estimation. Consequently, this significant gap needs to be filled and further research should be undertaken towards the integrated loss and risk assessment of tunnels and underground networks. This is the novelty of this study with important practical impact.

Under the above considerations, the aim of this study is twofold: (i) to develop a practical approach for probabilistic seismic loss assessment of circular tunnels and (ii) to examine the effects of salient parameters, such as soil conditions, tunnel buried depths, tunnel construction quality, or aging phenomena of the lining, on the seismic loss assessment at different scales, i.e. individual tunnel sections and metro lines. For this purpose, the approach for probabilistic seismic loss assessment of circular tunnels is firstly presented and employed on single tunnel segment in alluvial deposits, as well as on tunnel elements representative of the Shanghai Metro Lines 1 and 10, assuming various levels of seismic hazard. Limitations of the present study and further research efforts related to the more refined seismic loss assessment of tunnels are also discussed. The results of this study are beneficial for engineers, decision-makers, and infrastructure operators dealing with the resilience-based design and management of critical assets [38–40], The improved understanding and quantification of potential losses in case of earthquake events of different intensity, can support prevention, emergency, and recovery planning and enhance the seismic resilience of city infrastructure and communities.

2. Probabilistic seismic loss assessment framework

Fig. 1 summarizes the adopted framework in this study for the probabilistic seismic loss assessment of tunnels, used to examine the effects of salient parameters on the seismic losses. The framework includes the following three steps: (a) seismic hazard assessment, which can be performed based on available hazard curves for the site where the examined tunnel is located; (b) seismic vulnerability assessment by using appropriate fragility functions, which represent the degree of seismic damage under different levels of hazard intensities; (c) seismic direct economic loss assessment, which includes the quantification of the exceedance probability of different seismic losses, and the estimation of expected mean seismic loss. The former describes the exceedance probability of seismic loss under a given scenario of hazard intensity. In contrast, the latter describes the expected average seismic loss of the examined tunnels under various levels of hazard intensities. It is noted that the seismic direct economic loss in this study is associated with the repair cost after an earthquake event and is defined as a percentage of the initial construction cost of the damaged tunnel element. The details of these three steps are introduced in the subsequent sections.

2.1. Seismic hazard assessment—hazard curves

Seismic hazard and the required seismic hazard curves may be derived in different ways, for instance, through site-specific earthquake micro zonation investigations [41] or project-based seismic hazard analyses. It is recalled that seismic hazard curves are plots of the annual frequency of exceedance as a function of a seismic *IM* (e.g., the peak ground acceleration *PGA* or spectral acceleration). Generally, the peak ground acceleration (*PGA*) at the ground surface is most widely used to describe the seismic hazard intensity for the tunnels [42,43]. This analysis aims at defining the corresponding seismic hazard scenarios for a tunnel site that may be further used to evaluate the expected losses of the examined tunnel for these given scenarios (steps b and c). It is noted that the generation of the seismic hazard curve is quite complex, which should carefully deal with the factors of the faults and seismic sources on the site, the method of evaluating seismicity, among others. For simplification, the hazard analysis in this study is based on available hazard curves or other relevant studies for the examined tunnel sites. Site-specific seismic studies will be conducted in the future to obtain more appropriate seismic hazard curve for the examined tunnel sites.

2.2. Seismic vulnerability assessment—fragility functions

Fragility functions are generally employed in seismic vulnerability assessment of structures (tunnels herein). Fragility functions provide the conditional probability of a structure's likelihood to reach or exceed a specific level of damage under a given seismic *IM*. Fragility functions may be developed based on expert judgment, empirical approaches (e.g., statistical analysis of observations of the structure's response during past earthquakes), as well as numerically-based approaches, which have become popular in the last few years. In most studies, a lognormal probability distribution has been adopted to express fragility functions for tunnels in the form of fragility curves:

$$P\left[ds \geq ds_i | IM\right] = \Phi\left[\frac{In(IM) - In(IM_{mi})}{\beta_{tot}}\right] \tag{1}$$

where P[-] represents the conditional probability of reaching or exceeding a damaged state (ds) at a given *IM*; F(-) represents distribution function; IM_{mi} is the median value of *IM* corresponding to the i_{th} *ds, and* β_{tot} stands for the standard deviation, expressing the uncertainties related with fragility analysis. For the examined tunnel structures, the fragility curves are usually derived for minor (ds_1), moderate (ds_2), and extensive (ds_3) damage. The punctual probability w_i for each damage state (ds_i) can be derived based on the corresponding fragility curves. The punctual probability w_i for each damage state (ds_i) may be estimated by using the following equations:

$$\text{No damage}: w_0 = 1 - P\left[ds < ds_1 | IM\right] \tag{2}$$

$$\text{Minor damage}: w_1 = P\left[ds > ds_1 | IM\right] - P\left[ds > ds_2 | IM\right] \tag{3}$$

$$\text{Moderate damage}: w_2 = P\left[ds > ds_2 | IM\right] - P\left[ds > ds_3 | IM\right] \tag{4}$$

$$\text{Extensive damage}: w_3 = P\left[ds > ds_3 | IM\right] \tag{5}$$

where w_0, w_1, w_2, and w_3 refer to the corresponding punctual probability for no damage (ds_0), minor damage (ds_1), moderate damage (ds_2), and extensive damage state (ds_3); $P[ds > ds_j | IM]$ is the conditional probability of reaching or exceeding a damage state (ds) at a specific *IM* which may be obtained from Eq. (1).

2.3. Seismic loss assessment

The expected direct seismic losses of complex structures like a single tunnel line or tunnel lines of a metro system, which are examined herein, can be evaluated by identifying the potential damage states of the examined tunnels based on fragility functions and the associated repair cost for each damage state (ds) for different levels of seismic *IM*. The repair cost for each damage state may be estimated based on expert judgment or available data from repairs of similar structures during past earthquakes. Werner et al. [44] suggested a tunnel repair model based on data collected in the state of California. This model is based on the mean loss ratio (*LR*), which is described as the ratio of repair cost to the initial construction cost (*ICC*) of the tunnel element for each damage state (ds_i). In this study, the corresponding LR_i for none, minor, moderate, and extensive damage are assumed to equal 0, 0.10, 0.25, and 0.75,

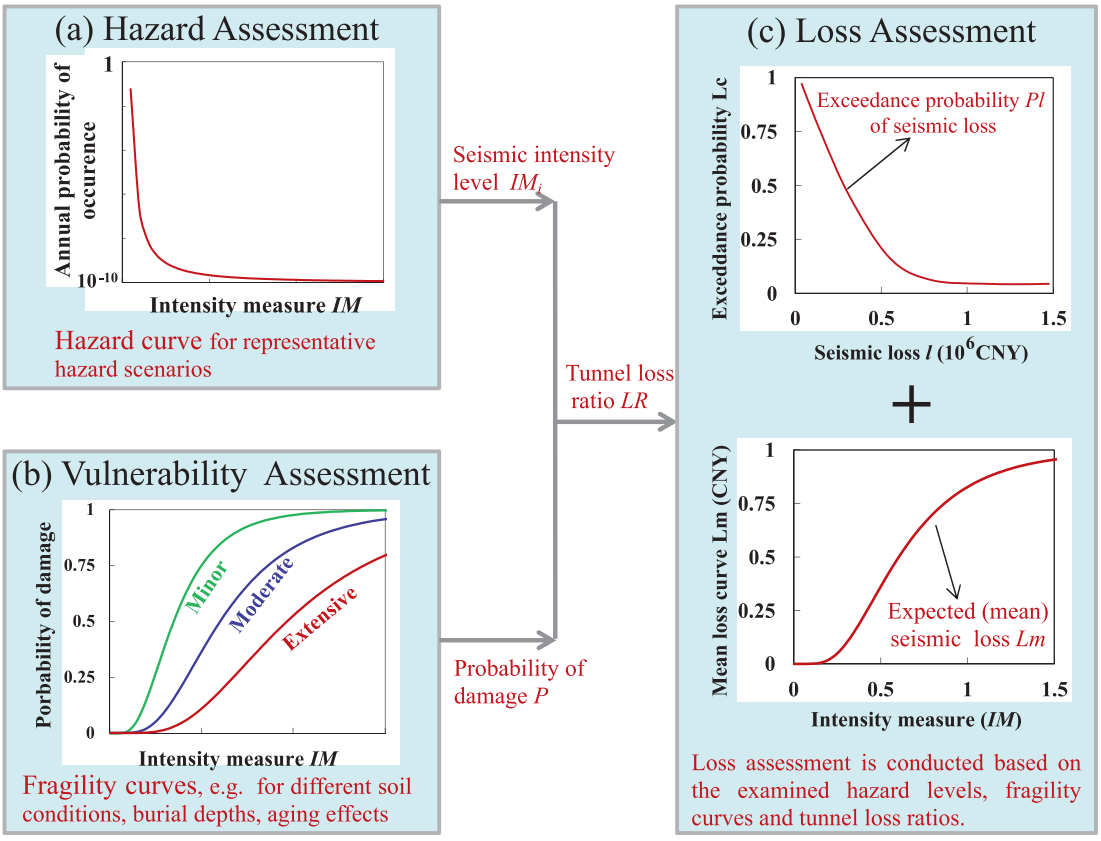

Fig. 1. Framework to assess the seismic loss of tunnels (*IM*: intensity measure; *l*: seismic loss; *P*: probability of damage; *LR*: loss ratio; *Pl*: exceedance probability of seismic loss; *Lm*: expected or mean seismic loss).

Table 1
Definitions of tunnel damage states and corresponding loss ratio (*LR*).

Damage states (*ds*)	Damage descriptions	Crack specification		Loss ratio (*LR*)
		Length (m)	Width (mm)	
None damage, ds_0	No cracking of the lining	-	-	0.00
Minor damage, ds_1	Minor cracking of the lining	<5	<3	0.10
Moderate damage, ds_2	Moderate cracking of the lining	5-10	3-30	0.25
Extensive damage, ds_3	Extensive cracking of the lining	>10	>30	0.75

respectively, as per Werner et al. [44] (Table 1). Herein, the adopted Loss Ratio (*LR*) presented in Table 1 are the same as the Repair Cost ratio presented in the original work [44]. The proposed Loss Ratio can be used for a preliminary application of probabilistic seismic loss assessment of tunnels. Moreover, it is noted that the various tunnel damage states are defined based on the reported cases of damage during past earthquakes [10,45], and the physical description of the damage states could be quantitatively described by the length and width of cracking of the lining, as shown in Table 1.

In engineering practice, the expected cost C_i to repair a certain damaged tunnel element under a certain damage state ds_i may be estimated by the length, and the initial construction cost (*ICC*) of the single tunnel segment (per unit length) as well as the *LR* mentioned above for different damage states, as shown below:

$$C_i = ICC \cdot LR_i \cdot n \tag{6}$$

where index i denotes the i_{th} damage state, C_i is the expected cost under i_{th} damage state, LR_i is the corresponding loss ratio in repairing the i_{th} damage state, and n represents the length of examined tunnel element. In this study, for the examined typical circular tunnel lining (i.e., prefabricated concrete segments, diameter d < 15 m, buried depth h < 40 m) with a longitudinal length of 1 m constructed by the shield tunnelling method, the initial construction cost is assumed to be 1,000,000 CNY [46], which only refers to the tunnel lining construction cost, and is the same for all examined soil conditions for a preliminary analysis. Moreover, it is noted that this study focuses on the direct economic cost caused by the repair of tunnel lining, while the potential economic cost of track, utilities, electrification, etc., are not considered herein.

The damage state of a structure for a given level of *IM* constitutes a random variable. Therefore, a sample of damage states for the examined tunnel element should be employed, by introducing a stochastic analysis, for instance, a Monte Carlo (MC) stochastic simulation (by Eqs. (2)-(5). Through this procedure, a sample of expected cost C_i can be obtained (by Eq. (6)). The Monte Carlo stochastic simulation is conducted as follows and the step-by-step procedure is shown in Fig. 2:

(a) A particular damage state i is determined for the examined tunnel element by comparing its w_i with a random number between 0 and 1.
(b) Based on the generated random damage scenario at each MC realization, the seismic loss of the whole examined tunnel system (assuming that the examined tunnel has k elements) is obtained through adding

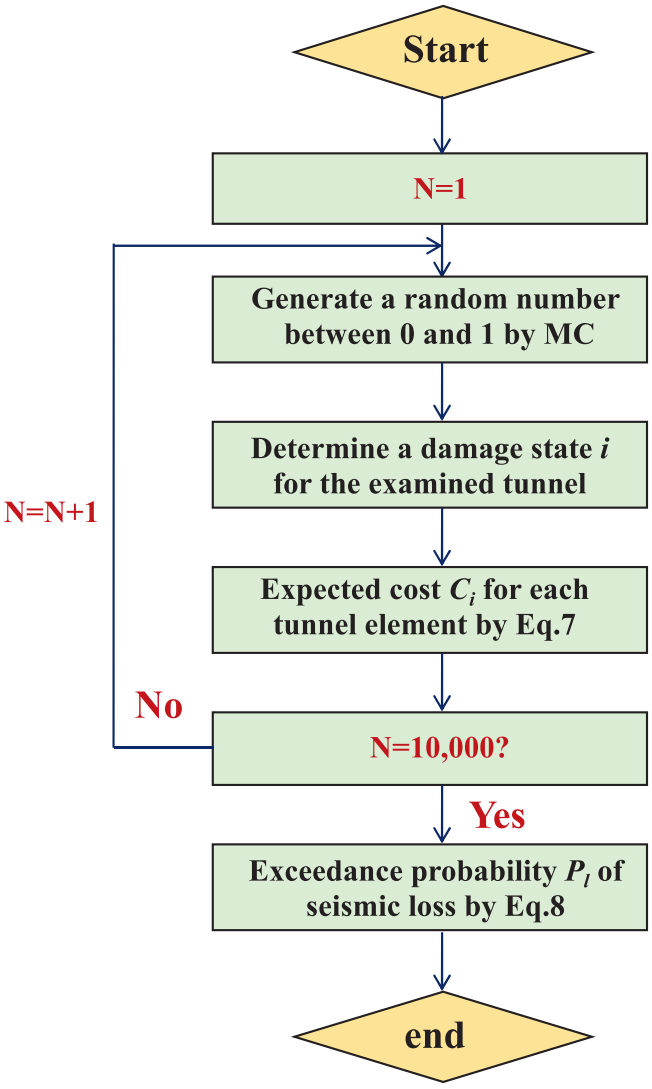

Fig. 2. Proposed Monte Carlo stochastic simulation procedure.

up the expected cost C_i for each tunnel element, as shown below:

$$l = \sum_{k=1}^{k} C_i \tag{7}$$

By running the MC simulation for many trials, e.g., 10,000 times or more, a large sample of potential total losses can be obtained for a specific level of *IM*=*im*. Thus, the exceedance probability *Pl* of seismic loss for a specific level of *IM*=*im* can then be represented as follows:

$$Pl(im, w) = p(l > x|\ im, w) \tag{8}$$

where *w* is the punctual probability that reflects the effect of seismic fragility of the examined structure. Based on the above discussion, the exceedance probability *Pl* may be determined by the seismic hazard level and the adopted fragility functions.

In addition to the exceedance probability *Pl* of seismic loss, the expected mean seismic loss *Lm* is adopted in this study as an additional loss metric of the examined tunnel systems, which is estimated based on Eq. (9) (assuming that the examined tunnel has *k* elements):

$$Lm(im, w) = \sum_{k=1}^{k} \sum_{i=0}^{4} C_i^k \cdot w_i \tag{9}$$

where *im* is the seismic hazard level, *k* denotes the total number of tunnel elements, C_i^k represents the expected cost to repair the certain tunnel element *k* under a certain damage state ds_i, and w_i represents the punctual probability of each damage state (ds_i).

3. Effects of salient parameters on seismic losses of tunnel segments and systems

The effects of salient parameters, such as the ground characteristics, the burial depth, and construction quality of the tunnel, as well as potential aging phenomena on the tunnel liners, on the seismic losses of tunnels, are examined in the following sections for representative circular tunnels under different seismic scenarios. This analysis includes two case studies: (i) a generic single tunnel lining segment with a unit length, and (ii) the Shanghai Metro Line 1 and Line 10.

3.1. Description of the adopted fragility functions

To examine the effects of some critical design factors on the seismic loss analysis of tunnels, this study adopted a set of fragility curves developed by authors' previous research [17,21,23]. More specifically, the fragility curves by Argyroudis and Pitilakis [17] are used to evaluate the seismic loss of shallow circular tunnels constructed in different soil conditions [47]. A set of fragility curves by Huang et al. [21] are applied to assess the seismic loss of tunnels with different buried depths. Additionally, to account for the effects of tunnel construction quality, as well as of potential aging phenomena of the liner due to corrosion, the fragility curves developed by Argyroudis et al. [23] for shallow circular tunnels in soil class C and D are used. Herein, the definition of tunnels with good or poor construction quality follows the scheme proposed by Argyroudis et al. [23]. The quality of tunnels are determined by the lining material properties. For the same site and design conditions, a good quality tunnel indicates it has a higher lining elastic modulus, while the poor quality tunnel indicates it has a lower lining elastic modulus. Moreover, the detailed information of the adopted size of the model, the density and elastic modulus, shear wave velocity distribution of the soil profile, the properties of the examined tunnels, as well as the development of numerical models can be further referred to the authors' previous work [17,21,23].

All the above-mentioned fragility curves are shown in Fig. 3. The required parameters to plot the fragility curves (i.e., median values of *IM* corresponding to minor, moderate, and extensive damage, as well as the standard deviation β_{tot}) are summarised in Table 2. In line with the work by Selva et al. [36], the fragility curves in terms of *PGA* are used to evaluate the probabilistic seismic loss assessment of tunnels under different damage states. In future work, the fragility curves in terms of *PGD* should be also adopted to improve the reliability of loss assessment results. It is noted that there exist some differences for the fragility curves of shallow tunnel in soil class D, as shown in Fig. 3(a) and Fig. 3(b). Specifically, a lower fragility is observed by Argyroudis et al. [23] compared with the work of Huang et al. [21]. Generally, the reason for these discrepancies is that the properties of the soil-tunnel system examined in the two studies are totally different, which ultimately results in significant different soil-tunnel response. More discussion about the reasons of these differences can also be checked in the authors' previous work [21].

3.2. Seismic loss assessment of a single tunnel segment

By adopting the fragility curves described in Table 2, and the tunnel repair model of Table 1, the seismic loss assessment framework, presented above, is initially applied on a single tunnel lining segment with a unit length considering different soil-tunnel configurations. The effects of crucial factors are presented and discussed thoroughly.

3.2.1. Effect of soil conditions on the seismic losses

To examine this effect, the soil-tunnel configurations examined by Argyroudis and Pitilakis [17], and the relevant fragility functions

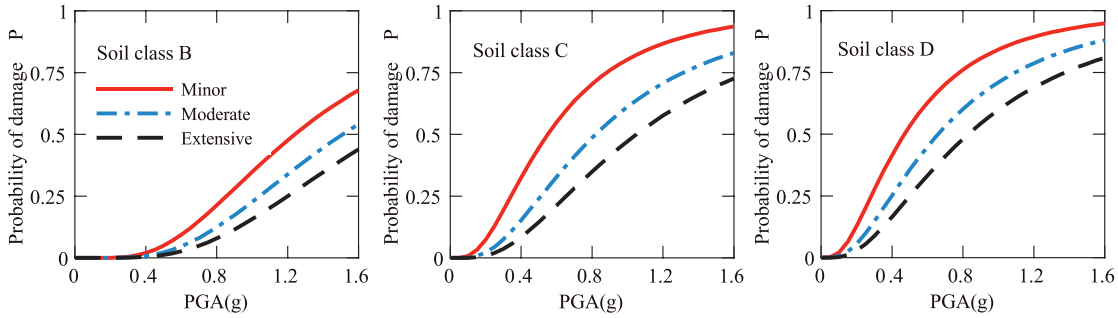

(a) Fragility curves of shallow circular tunnels provided by Argyroudis and Pitilakis[17].

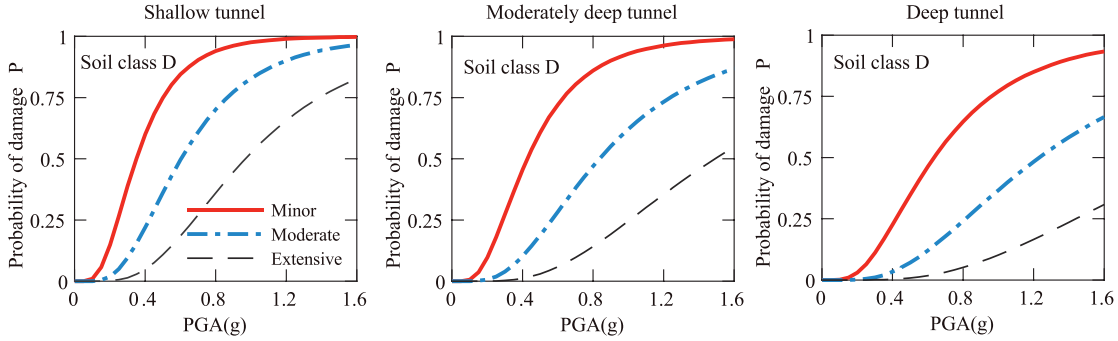

(b) Fragility curves of tunnels with different buried depths developed by Huang et al.[21].

Fig. 3. Fragility curves developed by authors' previous work and used herein. (a) Fragility curves of shallow circular tunnels provided by Argyroudis and Pitilakis [17]. (b) Fragility curves of tunnels with different buried depths developed by Huang et al. [21]. (c) Time-dependent fragility curves for shallow circular tunnels in soil class C by Argyroudis et al. [23]. (d) Time-dependent fragility curves for shallow circular tunnels in soil class D by Argyroudis et al. [23].

Table 2
Parameters of the adopted fragility curves in this work.

Reference	Tunnel typology	Soil class	Tunnel service time (years)	Minor IM_1 (g)	Moderate IM_2 (g)	Extensive IM_3 (g)	b_{tot}
Argyroudis and Pitilakis [17]	Shallow tunnel, buried depth h =10 m, diameter d= 10 m	B	-	1.240	1.510	1.740	0.550
		C	-	0.550	0.820	1.050	0.700
		D	-	0.470	0.660	0.830	0.750
Huang et al. [21]	Shallow tunnel, buried depth h =9 m, diameter d= 6.2 m	D	-	0.350	0.604	0.968	0.533
	Moderately deep tunnel, buried depth h =20 m, diameter d= 6.2 m		-	0.427	0.836	1.491	0.580
	Deep tunnel, buried depth h =30 m, diameter d= 6.2 m		-	0.635	1.231	2.177	0.613
Argyroudis et al. [23]	Shallow tunnel, buried depth h =10 m, diameter d= 6 m, good construction quality	C	0	0.770	1.040	1.280	0.680
			50	0.730	1.010	1.250	0.710
			75	0.680	0.960	1.190	0.770
			100	0.640	0.910	1.140	0.83
		D	0	0.510	0.890	1.220	0.610
			50	0.470	0.850	1.190	0.630
			75	0.410	0.790	0.740	0.660
			100	0.350	0.740	1.080	0.690
	Shallow tunnel, buried depth h =10 m, diameter d= 6 m, poor construction quality	C	0	0.690	0.950	1.170	0.780
			50	0.650	0.910	0.870	0.820
			75	0.610	0.870	1.100	0.880
			100	0.580	0.830	1.050	0.940
		D	0	0.250	0.610	0.910	0.760
			50	0.200	0.560	0.870	0.800
			75	0.150	0.510	0.820	0.850
			100	0.100	0.450	0.760	0.920

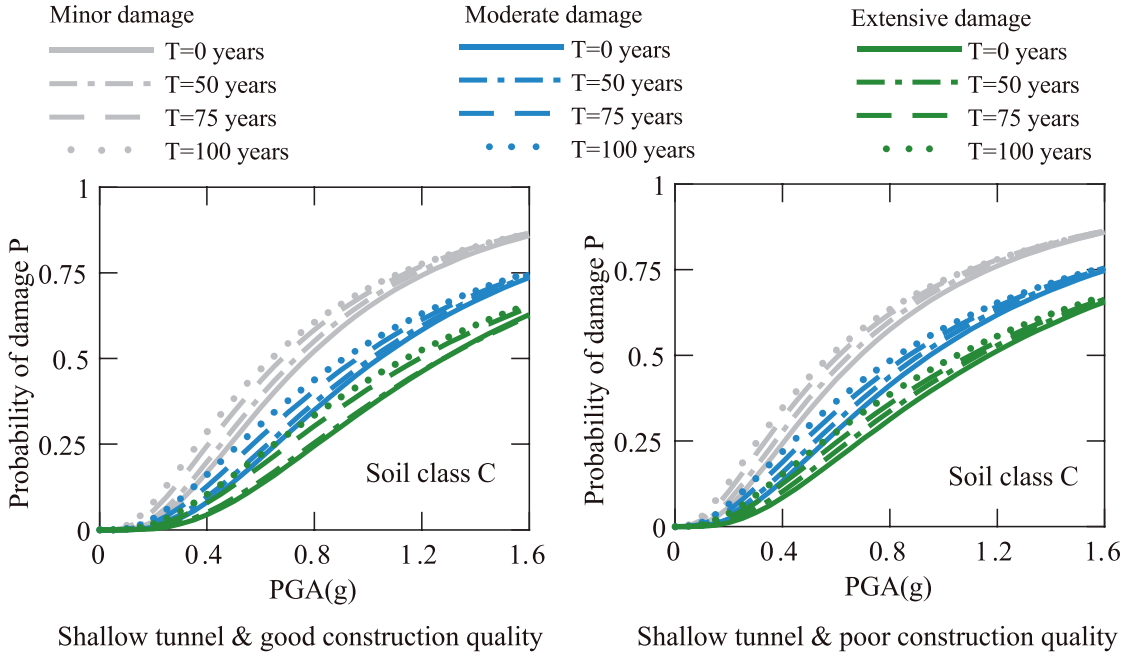

(c) Time-dependent fragility curves for shallow circular tunnels in soil class C by Argyroudis et al.[23].

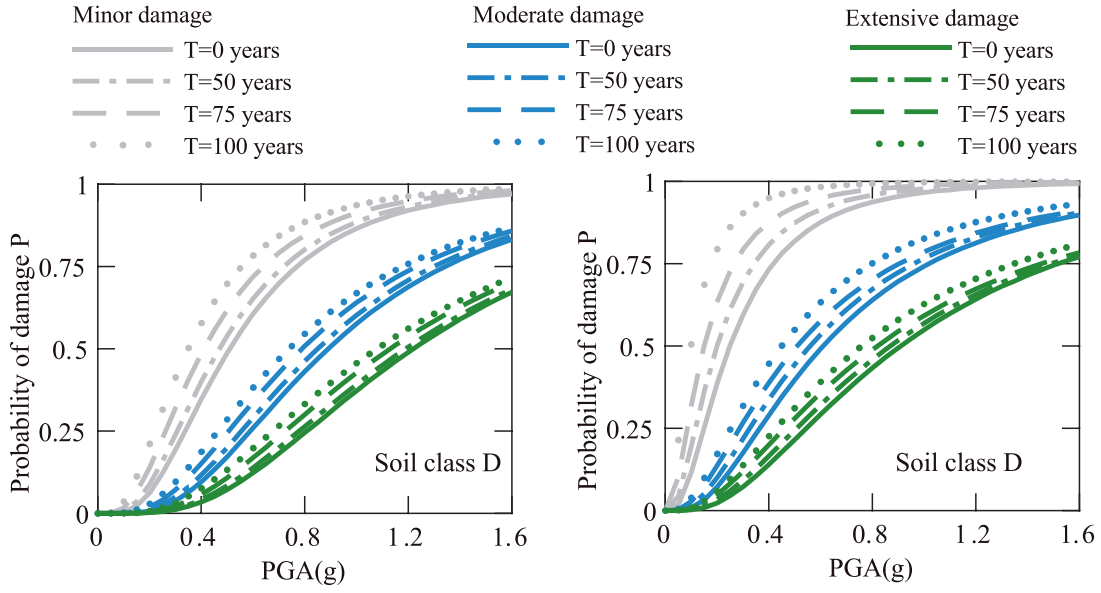

(d) Time-dependent fragility curves for shallow circular tunnels in soil class D by Argyroudis et al.[23].

Fig. 3. Continued

(Fig. 3a), are adopted in the seismic loss assessment, which is performed for distinct seismic hazard levels. It is recalled that the configurations refer to a circular tunnel with a diameter $d = 10$ m, embedded at a burial depth $h = 10$ m in soil class B, C, and D, according to Eurocode 8 [47].

Fig. 4 presents the exceedance probability *Pl* of seismic loss for the examined shallow tunnels in soil class B, C, and D under three seismic hazard intensities, i.e., *PGA* equals 0.2, 0.6, and 1.0 g. The reason for the flat segment lines in this figure is due to the way that loss values are estimated using an average loss ratio, as in Table 1. The computed exceedance probability *Pl* generally decreases with the increase of seismic losses for all the examined cases. In addition, for a given level of seismic losses, the exceedance probability *Pl* increases with the increased seismic hazard level. For a given level of seismic hazard and seismic losses, the exceedance probability *Pl* decreases with the "quality" of the soil surrounding the examined tunnel segment (i.e., increase of the stiffness and strength of soil or from soil class D to B). Assuming a *PGA*=0.6

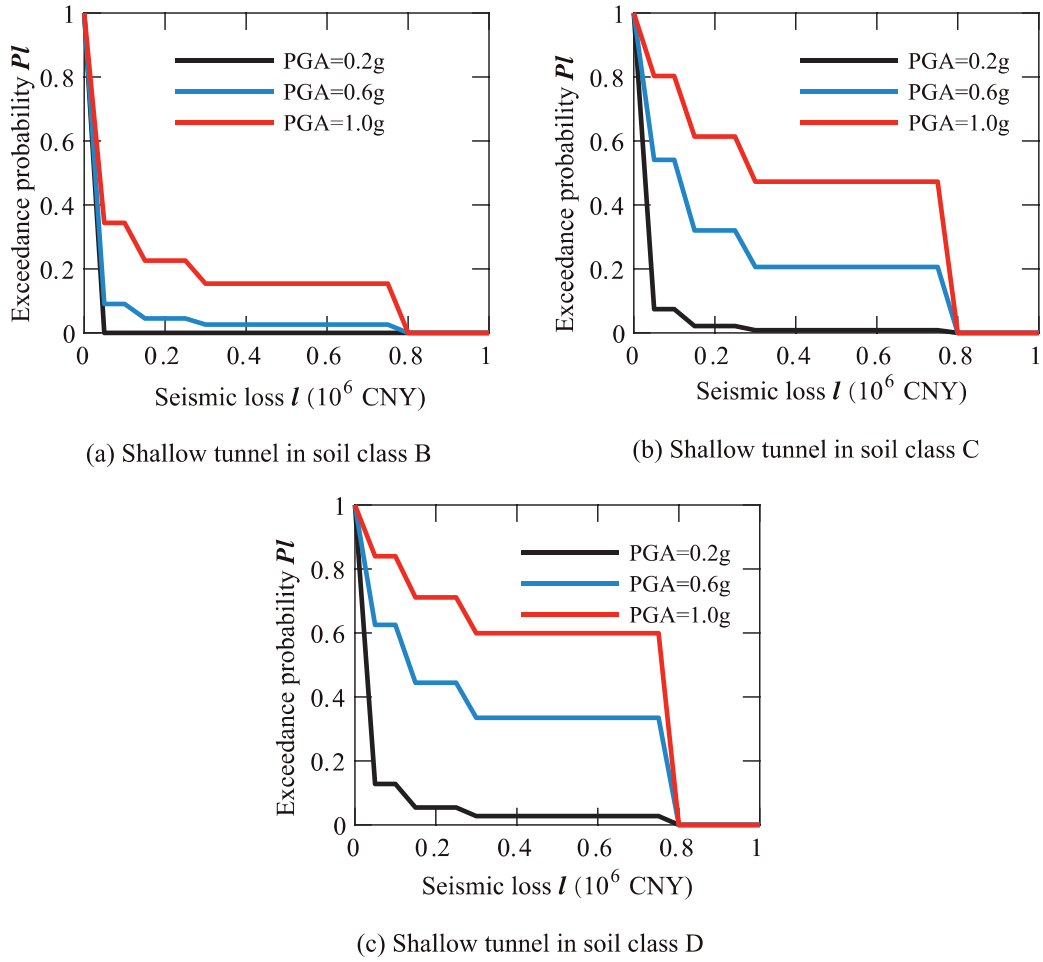

Fig. 4. Exceedance probability *Pl* of seismic loss for tunnels in different soil conditions.

g and a level of seismic losses l=0.6·10^6 CNY as an example, the exceedance probability *Pl* of the sections equals 0.026, 0.206, and 0.335 for soil class B, C, and D, respectively. It can be inferred from the above results that the differences in the calculated exceedance probability *Pl* of a tunnel segment in different soil conditions could be larger than 1100%.

The expected mean seismic losses *Lm*, of the examined soil-tunnel configurations, are calculated according to Eq. (9). Fig. 5 shows the evolution of the estimated mean seismic losses *Lm* for different levels of seismic hazard, the latter expressed in terms of *PGA*. Evidently, the mean seismic losses L_m of examined configurations increase remarkably with the increase of the seismic hazard level. Additionally, for a given level of seismic intensity, the mean seismic losses *Lm* increase with the decrease of the "quality" of soil conditions (i.e., from soil class B to D). Summarizing, the effect of soil conditions on the seismic loss assessment of tunnels is significant, and the tunnel embedded in soft soil deposits generally is expected to sustain higher seismic loss due to e.g. larger deformations and bending moments developed at critical locations of the tunnel lining [21,23].

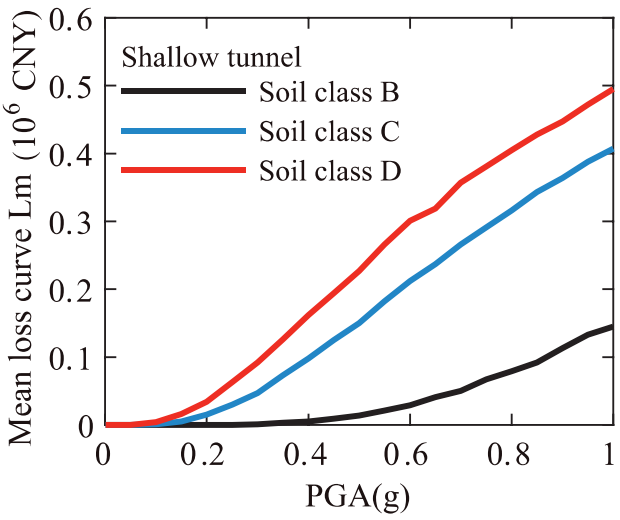

Fig. 5. Expected mean seismic loss *Lm* of the shallow tunnel in different soil conditions.

3.2.2. *Effect of burial depth on the seismic losses*

Previous studies (e.g., [48]) have demonstrated the critical effect of burial depth of the tunnels or other underground structures on the seismic response of the soil-structure configuration. Therefore, examining the burial depth's impact on seismic losses of tunnels is essential. The assessment herein refers to the tunnel segments corresponding to the soil-tunnel configurations examined by Huang et al. [21]. In particular, a tunnel segment embedded in different burial depths in soil class D is used as a case study, with the relevant fragility curves proposed by the researchers, as shown in Fig. 3b.

Fig. 6 illustrates the exceedance probability *Pl* of seismic losses for the examined configurations under three seismic hazard levels. For a given seismic hazard level, the exceedance probability *Pl* decreases with

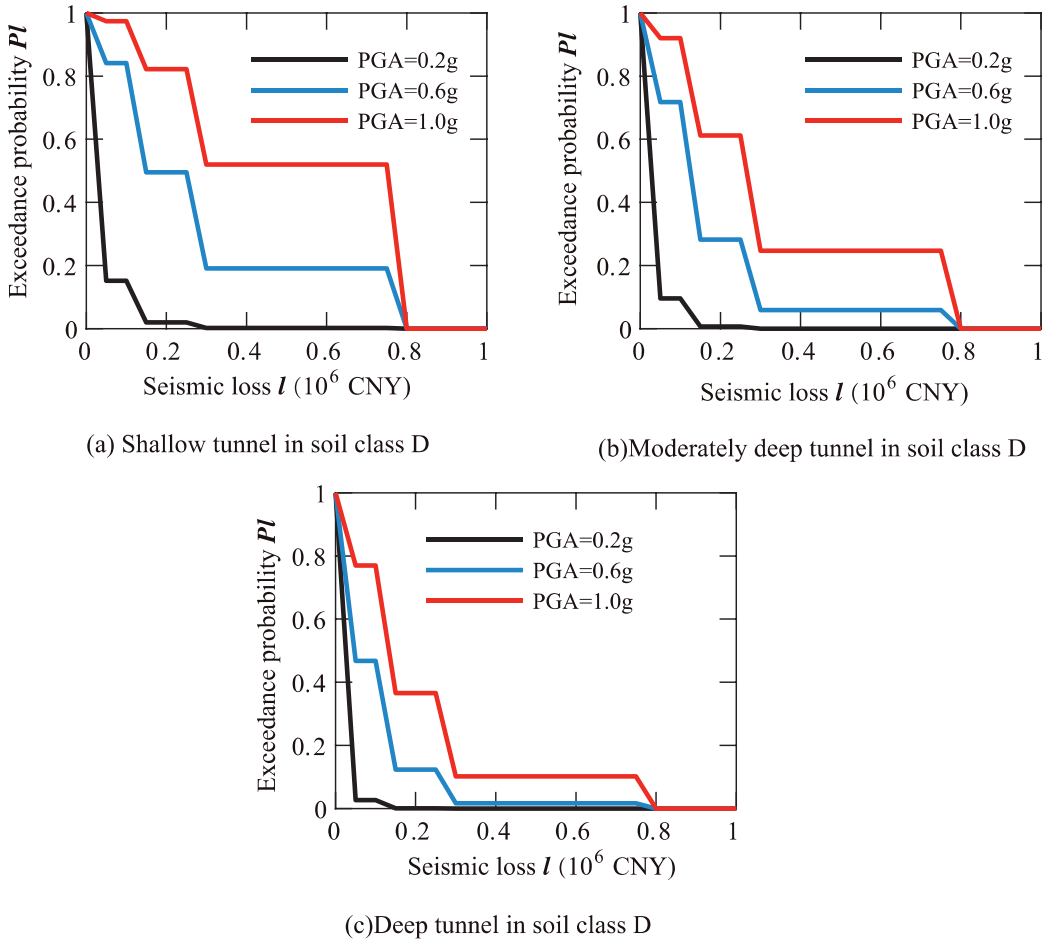

Fig. 6. Exceedance probability *Pl* of seismic loss for tunnels with different buried depths.

the increase of seismic losses for all the examined burial depths. Moreover, for a given level of seismic losses, the exceedance probability *Pl* increases with the increase of seismic hazard level (i.e., as *PGA* changes from 0.2g to 1.0g). For a given level of seismic hazard and seismic losses, the exceedance probability *Pl* of the examined tunnel decreases with the increase of the burial depth of the tunnels (i.e., from the shallow tunnel to the deep tunnel). Using *PGA*=1.0g and seismic loss l=0.6·10^6 CNY as an example, the exceedance probability *Pl* of the tunnel equals 0.520, 0.247, and 0.102 for the shallow, moderately deep tunnel, and deep tunnels, respectively. The differences in the estimated exceedance probability *Pl* for the examined tunnels embedded in various burial depths are as high as 400%.

Fig. 7 quantifies the mean seismic loss *Lm* of the examined tunnels for different burial depths under and different levels of seismic hazard. As expected, *Lm* increases gradually with the increase of seismic intensity. Lower values of mean seismic losses are calculated for the deep tunnel case compared to the shallower ones. The differences on *Lm* are higher for higher seismic intensities (*PGA*>0.5g). On the contrary, for *PGA* levels up to 0.2g, the effect of burial depth on the expected mean seismic loss is less important. For example, for a *PGA* equal to 0.20 g, the expected mean seismic loss value is equal to 0.018·10^6, 0.011·10^6, and 0.004·10^6 CNY for the shallow, moderately deep, and deep tunnels, respectively. For a *PGA* equal to 0.80 g, the expected mean seismic loss is increased significantly to 0.379·10^6, 0.227·10^6, and 0.126·10^6 CNY for the shallow, moderately deep, and deep tunnels, respectively. Generally, the seismic losses *Lm* are found to increase for the shallower section, particularly for higher seismic intensities (i.e., for *PGA* > 0.2g).

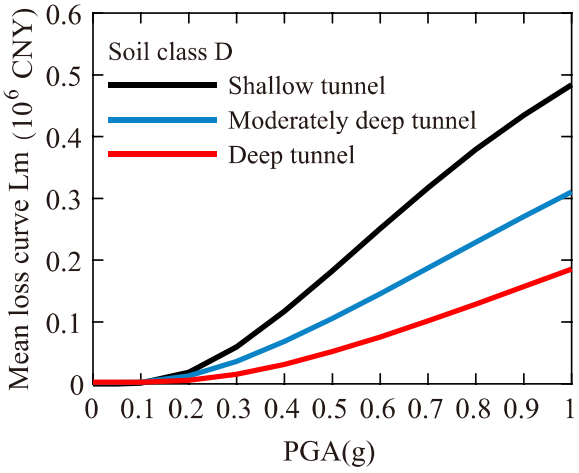

Fig. 7. Expected mean seismic loss *Lm* for tunnels with different buried depths.

3.2.3. *Effect of tunnel construction quality on the seismic losses*

To examine the effect of tunnel's construction quality on seismic losses, tunnel segments corresponding to the soil-tunnel configurations examined by Argyroudis et al. [23], were adopted herein. Two tunnel segments are adopted corresponding to good or poor construction quality (as per [23]). The tunnels are assumed to be embedded in soil class C or soil class D. The fragility curves, proposed by Argyroudis et al.

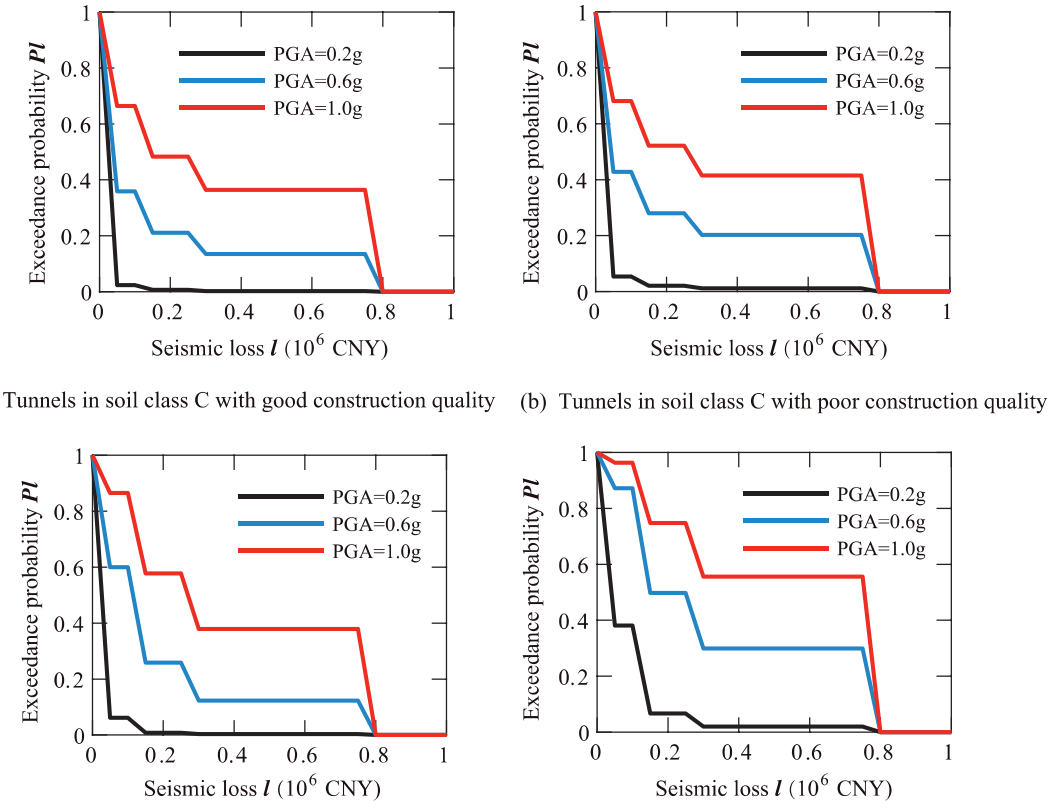

(a) Tunnels in soil class C with good construction quality (b) Tunnels in soil class C with poor construction quality

(c) Tunnels in soil class D with good construction quality (d) Tunnels in soil class D with poor construction quality

Fig. 8. Exceedance probability *Pl* of seismic loss for the shallow tunnel with different construction quality.

[23] for the initial operation (i.e., for T=0 years with aging effects being disregarded), as shown in Figs. 3 (c) and (d), are adopted in the subsequent seismic loss assessment investigations.

Fig. 8 illustrates the exceedance probability *Pl* of seismic losses estimated for the examined tunnel segments (tunnels of good or poor construction quality) for three seismic hazard levels. For a given level of seismic hazard intensity and a given level of seismic losses, the exceedance probability *Pl* of the examined tunnel with good construction quality is lower than the tunnel with poor construction quality. Assuming the scenario of a *PGA*=0.6g and seismic losses l=0.6·10^6 CNY, and that the tunnel is embedded in soil class C as an example, the exceedance probability *Pl* is equal to 0.135 and 0.203 for the tunnel with good or poor-quality construction, respectively. For the examined tunnel segments, the differences in the calculated exceedance probability *Pl* of the tunnels due to different construction quality may be as high as 50%.

The estimated mean seismic loss *Lm* values, for the examined tunnels with good or poor construction quality, are plotted comparatively in Fig. 9. For a given seismic intensity and a given soil, the tunnel's expected mean seismic loss with poor construction quality is lower than the one estimated for the tunnel with poor construction quality. Additionally, by comparing Fig. 9 (a) and (b), it is observed that the effect of the construction quality is more significant for softer soil deposits, i.e., soil class D compared to soil class C. Indeed, assuming a *PGA* equal to 0.6 g and the tunnels in soil class C, *Lm* equals 0.131·10^6 and 0.181 ·10^6 CNY for the tunnels with good or poor construction quality, respectively. On the contrary, for a *PGA* = 0.6 g and tunnels built in soil class D, *Lm* is increased to 0.166·10^6 and 0.306·10^6 CNY for tunnels with good or poor construction quality, respectively. Summarizing, the effect of construction quality on the seismic loss assessment of tunnels is essential, particularly for cases where the tunnel is embedded in soft soil deposits.

3.2.4. *Effect of aging phenomena of the liner on the seismic losses*

Tunnels are generally built as long-term (e.g., over 100 years) service structures. Nevertheless, the seismic performance of tunnel structures would degrade slowly as their service time increases, owing to different aging phenomena, such as corrosion of steel bars or joints. In this context, the potential aging phenomena of the liner may affect the seismic losses of tunnels. To examine this effect, tunnel segments corresponding to the soil-tunnel configurations examined by Argyroudis et al. [23], i.e., shallow circular tunnels built in soil class C (Fig. 3c) and D (Fig. 3d), were employed in a seismic loss assessment investigation.

Four typical service years, including 0 years, 50 years, 75 years, and 100 years, were considered by Argyroudis et al. [23]. The estimated exceedance probability *Pl* of seismic loss for the examined circular tunnels in soil class D with good construction quality are shown in Fig. 10, corresponding to three seismic hazard levels. For a given level of seismic intensity and a given level of seismic losses, the exceedance probability *Pl* of the examined tunnel increases with the increase of service years (due to the deteriorating effect of liner corrosion on the seismic vulnerability of the tunnel). For a *PGA*=0.6g and a scenario of seismic losses l=0.6·10^6 CNY, the exceedance probability *Pl* equals 0.123, 0.132, 0.165, and 0.196 for 0 years, 50 years, 75 years, and 100 years, respectively. The above comparison, which reveals differences higher than 59% between examined scenarios of service years, demonstrates the effect of deteriorating corrosion phenomena of liner on the seismic loss estimation.

Figs. 11(a) and (b) present the mean seismic losses *Lm*, estimated for the examined cases, for different levels of seismic intensity and distinct scenarios of tunnel service time for the examined tunnel segments, corresponding to the tunnel configurations with good or poor construction quality, adopted by Argyroudis et al. [23]. Seismic loss *Lm* of the examined tunnel segment is found to increase with increasing years of service for investigated configurations. Indeed, higher values of *Lm* are calcu-

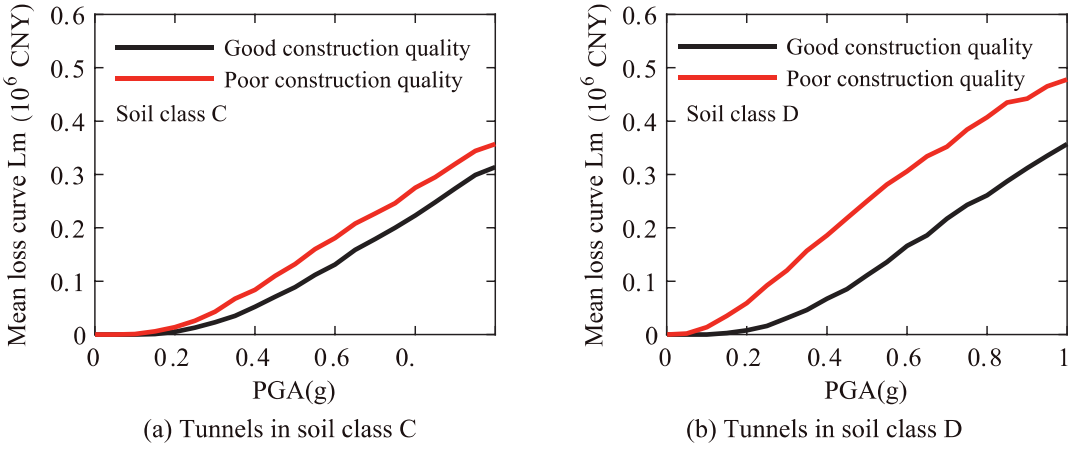

Fig. 9. Expected mean seismic loss *Lm* of tunnels with different construction quality.

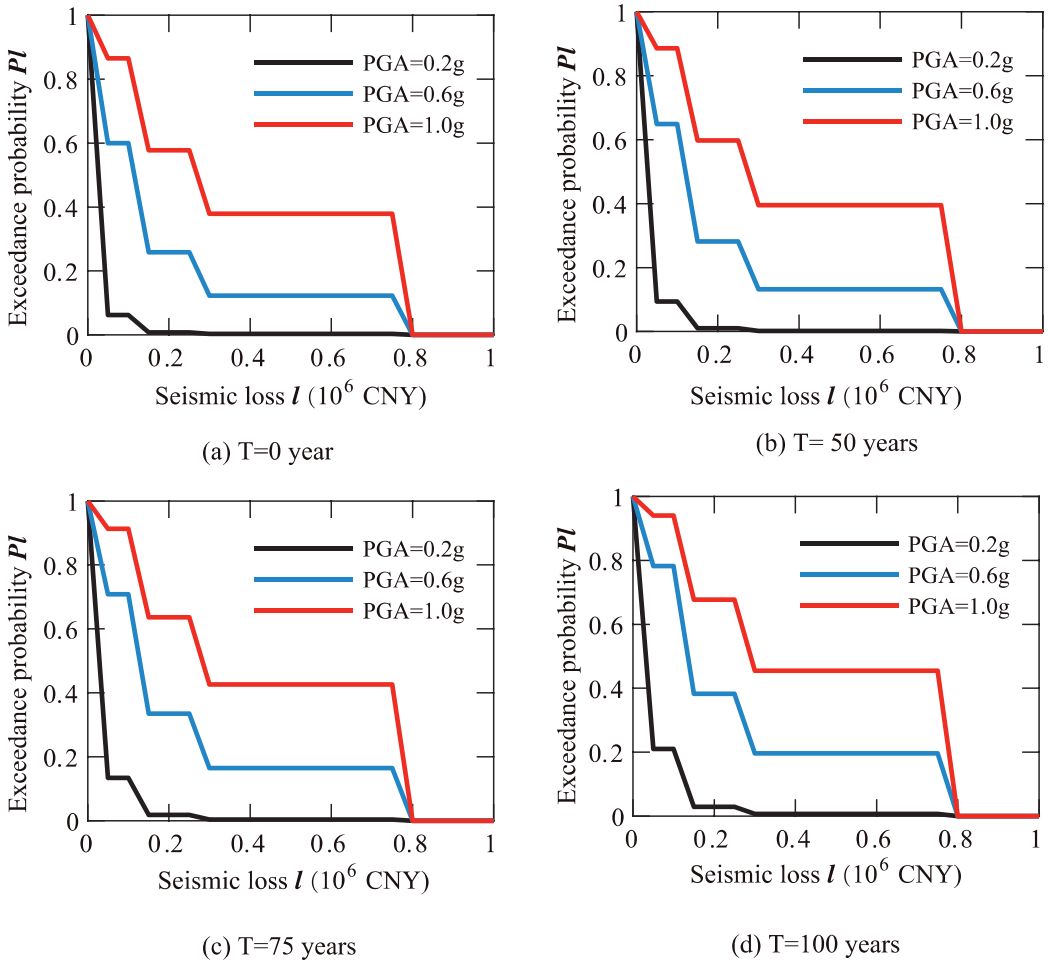

Fig. 10. Exceedance probability *Pl* of seismic loss for the shallow tunnel with good construction quality considering different service years.

lated for a service time of *T*=100 years compared to the ones estimated for *T*= 0 years, etc. This result indicates that the mean seismic losses of tunnels are expected to increase with growing service time, due to the increasing deterioration phenomena (mainly due to corrosion) on the tunnel liner.

According to the analyses, all salient parameters discussed in this paper have, as expected, a significant impact on the seismic loss assessment of tunnels. The value of the analysis performed is that these effects have been not only specified but also quantified in terms of losses, which may improve considerably the design by performing cost-benefit analyses to assess the benefits of different design solutions and to evaluate the best retrofits solutions based on risk-based seismic life-cycle costs and cost-benefit analysis upgrading in that way the resilience of the system.

4. Application of seismic loss assessment framework in a real case study: Shanghai Metro Lines 1 and 10

The above sections examined the effects of salient parameters on the assessment of seismic losses of tunnels, using idealized soil-tunnel configurations. To further explore the seismic losses of operated metro

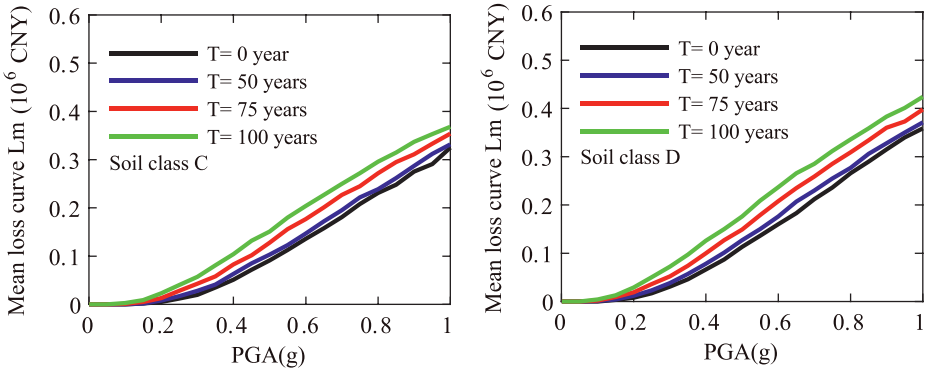

(a) Shallow tunnel with good construction quality

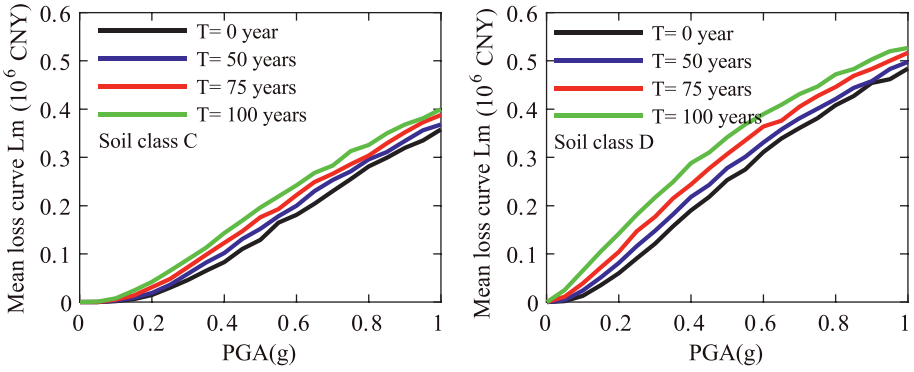

(b) Shallow tunnel with poor construction quality

Fig. 11. Expected mean seismic loss *Lm* of tunnels considering different service years.

Table 3
Typical soil properties of site for Shanghai Metro line 1.

Soil layer	Thickness(m)	Soil type	Unit wright (kg·m^{-3})	Shear wave velocity (m·s^{-1})	Cohesion (kPa)	Fraction angle (°)
1	8	Silty clay	1900	122	16.4	14
2	10	Silt	2000	164	22.0	24
3	6	Silty clay	1900	242	18.6	20
4	12	Clay	2000	320	23.0	26
5	12	Silty clay	1900	386	26.0	24
6	5	Sand	2000	450	0	36

lines in a city, the framework presented in Section 2 is applied for the assessment of a real metro system, i.e., Shanghai Metro Lines 1 and 10. The approach is applied throughout the length of the examined metro lines.

The examined Metro Lines 1 and 10 are all built in typical Shanghai soft clay, which has average shear wave velocities Vs_{30} about or lower than 200 m/s and can be classified in soil class D according to Eurocode 8 [48]. Moreover, the tunnel liners have the same dimensions and mechanical characteristics, i.e., a tunnel diameter of 6.2m and a lining thickness of 0.35m, as the one studied by Huang et al. [21]. Fig. 12 provides maps of the examined Shanghai Metro Lines 1 and 10.

The Shanghai Metro Line 1, built in 1994, consists of 13 stations between Jiangjing Action Park Station and Shanghai Railway Station, and has a full length of 16,365 m. A total of 12 different tunnel elements, i.e., from tunnel element ① to tunnel element ⑫, as well as their corresponding lengths, are shown in Fig. 12(a). The typical soil physical properties of site for Shanghai Metro line 1 is shown in Table 3. The tunnels along the Line 1 are of circular shape and are shallow buried in soft soils (the equivalent of soil class D of Eurocode 8) at a burial depth of fewer than 9 m below the ground surface. In this context, the fragility curves for shallow tunnels in clayey soil deposits proposed by Huang et al. [21] are used in the seismic loss assessment of Shanghai Metro Line 1.

The Shanghai Metro Line 10 was built in 2010. It consists of 19 stations from Hongqiao Road Station to Xinjiangwancheng Station, and its full length is 17,452 m. A total of 18 different tunnel elements, i.e., from tunnel element ① to tunnel element ⑱, as well as their corresponding lengths, are shown in Fig. 12(b). The typical soil physical properties of site for Shanghai Metro line 10 is shown in Table 4. The tunnels along Line 10 are characterized as either shallow (a full length of 2,733m), moderately deep (a full length of 12,464 m), or deep (a full length of 2,255 m) and are crossing again soft clayey soils (the equivalent of soil class D). More specifically, tunnel elements ①, ④, and ⑱ are classified into shallow tunnels, while tunnel elements ⑦ and ⑧ are classified into deep tunnels. In contrast, the other tunnel elements are all classified into moderately deep tunnels. Therefore, the fragility curves for shallow, moderately deep, and deep tunnels in clayey proposed by Huang et al. [21] are used in this case.

The exceedance probability *Pl* of seismic loss and the mean seismic loss *Lm* were estimated as per Figs. 13 and 14 for the two metro lines. Based on Figs. 13(a) and 14(a), for a given seismic hazard intensity, the exceedance probability *Pl* decreases with the increase of the seismic

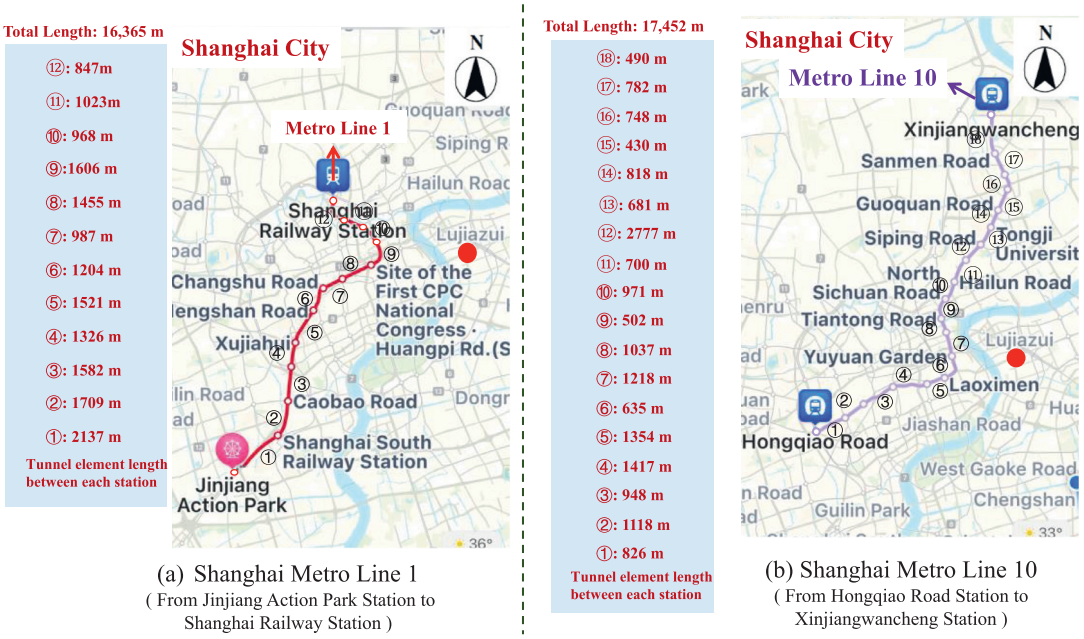

(a) Shanghai Metro Line 1
(From Jinjiang Action Park Station to Shanghai Railway Station)

(b) Shanghai Metro Line 10
(From Hongqiao Road Station to Xinjiangwancheng Station)

Fig. 12. Examined Shanghai Metro Lines 1 and 10 with circular cross-section built in soil class D [47] (CEN, 2004). Note: figures are not in scale.

Table 4
Typical soil properties of site for Shanghai Metro line 10.

Soil layer	Thickness(m)	Soil type	Unit wright (kg·m^{-3})	Shear wave velocity (m·s^{-1})	Cohesion (kPa)	Fraction angle (°)
1	3.0	Silty clay	1865	113	7.3	18.8
2	1.3	Silty clay	1814	119	15	19.0
3	2.3	Silt	1896	150	3.8	23.3
4	5.4	Clay	1743	153	11.4	19.0
5	6.4	Silty clay	1722	162	13.6	18.0
6	6.3	Silty clay	1824	188	15.8	18.0
7	4.8	Clay	1900	227	45	17.0
8	30.5	Clay	1936	277	5	20.0
9	10.0	Clay	1906	301	15	23.0
10	15.0	Sand	1987	385	0	35.0
11	15.0	Sand	2000	413	0	35.0

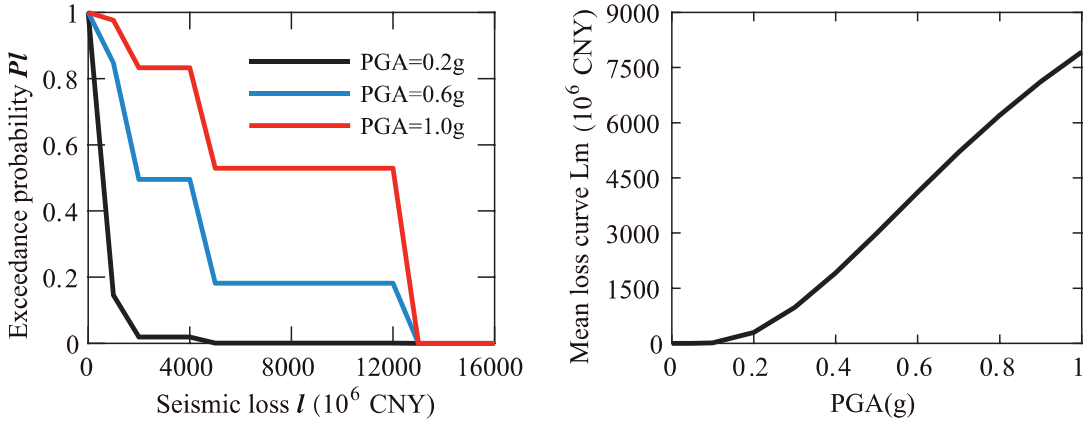

(a) Exceedance probability *Pl* of seismic loss

(b) Expected (mean) seismic loss *Lm*

Fig. 13. Seismic loss assessment of Shanghai Metro Line 1.

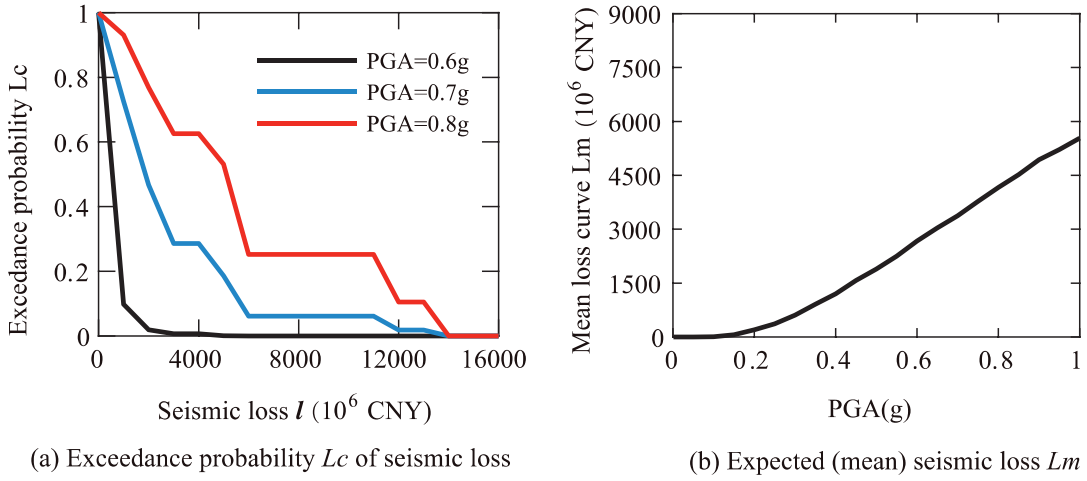

(a) Exceedance probability *Lc* of seismic loss (b) Expected (mean) seismic loss *Lm*

Fig. 14. Seismic loss assessment of Shanghai Metro Line 10.

loss values for both examined metro lines. On the other hand, for a given level of seismic losses, the exceedance probability *Pl* increases with the increase of the seismic hazard intensity (i.e., as *PGA* changes from 0.2 g to 1.0g). Assuming a scenario of seismic losses l=4·10^9 CNY as an example, for the Shanghai Metro Line 1, the corresponding exceedance probability *Pl* for *PGA* of 0.2, 0.6, and 1.0 g is equal to 0.019, 0.495, and 0.833. For the same assumptions, the corresponding exceedance probability *Pl* for the Shanghai Metro Line 10, equals 0.007, 0.286, and 0.626, for *PGA* of 0.2, 0.6, and 1.0 g, respectively.

The mean seismic losses *Lm* estimated for different levels of seismic intensity for Shanghai Metro Lines 1 and 10 are shown in Figs. 13(b) and 14(b), respectively. As expected, *Lm* increases gradually with the increase of seismic intensity. Indeed, for a *PGA* is equal to 0.40 g, the mean seismic loss value equals 1.917·10^9 and 1.203·10^9 CNY for Shanghai Metro Lines 1 and 10, respectively. However, when a *PGA* increases to 0.80 g, the expected mean seismic loss will increase by more than two times, i.e., 6.207·10^9 and 4.158·10^9 CNY for Lines 1 and 10, respectively. These results indicate that a high seismic ground shaking can lead to an exceptionally significant economic loss.

Additionally, the analysis reveals a higher mean seismic loss *Lm* for the examined Shanghai Metro Line 1 compared to that of Shanghai Metro line 10, even though the total length of Line 1 (i.e., 16,365 m) is shorter than Line 10 (i.e., 17,452 m). The main reason for this observation is the lower burial depth of the tunnels in Shanghai Metro Line 1.

Moreover, for different tunnel elements in the same metro line, their seismic loss estimation may be different, depending on the burial depth, soil conditions, or lengths of the examined sections. Taking seismic intensity *PGA*= 0.6g as an example, Figs. 15 and 16 show the distribution of the estimated expected mean seismic losses *Lm* along different tunnel elements of Shanghai Metro Line 1 and 10, respectively.

It is noted that the tunnel elements of Shanghai Metro Line 1 are all buried in the same soil conditions and classified as shallow tunnels, and their seismic loss assessment is generally determined by their tunnel element length. As can be seen in Fig. 12(a), tunnel element ① has the longest length, while tunnel element ⑫ has the shortest length. Accordingly, it can be observed in Fig. 15 that, among different tunnel elements of Shanghai Metro Line 1, tunnel element ① would have the highest seismic loss, i.e., 536.46·10^6 CNY, followed by tunnel elements ② and ⑨. Their corresponding seismic loss is 429.02·10^6 and 403.16·10^6 CNY, respectively, which are slightly lower than that for tunnel element ①. At the same time, the lowest seismic loss is observed for tunnel element ⑫, i.e., 212.63·10^6 CNY.

Additionally, it is worth noting that the tunnel elements of Line 10 are all buried in the same soil conditions and can be classified as shallow, moderately deep, and deep tunnels, respectively. In this regard, their seismic loss assessment is generally determined by their tunnel element length and burial depths. More information about different tunnel elements can be checked in Fig. 12(b). Generally, the comparisons in Fig. 16 suggest that tunnel element ⑫ has the highest seismic loss, i.e., 396.03·10^6 CNY. among others, because it has the longest tunnel length of 2777 m. Tunnel elements ① and ④ are observed to have the second and third highest seismic loss, with the corresponding *Lm* equal to 352.97.03·10^6 and 205.76·10^6 CNY, respectively. In contrast, Tunnel element ⑮ is found to have the lowest seismic loss of 61.32·10^6 CNY among the other tunnel elements.

The various components in the proposed seismic loss assessment framework, e.g., fragility curves, loss ratios, and tunnel initial construction cost, generally may have a high degree of uncertainty. Among them, the uncertainty from the selection of the appropriate fragility curves, which also reflect the actual conditions of a structure, i.e., a tunnel line, in this case, is essential [49–51].

To highlight the effect of this uncertainty, the mean seismic losses *Lm* of Shanghai Metro Line 1 was further studied using two different sets of fragility curves, i.e., the analytical fragility functions provided by Argyroudis et al. [23], and Huang et al. [21]. It is noted that the latter, which are particularly derived for the Shanghai Metro system, may be considered more appropriate for this analyzed case compared to the generic fragility curves proposed by Argyroudis et al. [23].

The results are shown in Fig. 17. Generally, it is found that the expected mean seismic loss *Lm* of Shanghai Metro Line 1 using generic fragility curves (i.e., [23]) is evidently lower than the one based on Huang et al. [21]. It is an important observation indicating that the use of fragility curves that do not correspond as close as possible to the specific typology of the examined structure may result in an underestimation of direct seismic loss, as observed herein for the Shanghai Metro Line 1. Taking *PGA*= 0.6g as an example, the expected mean seismic loss *Lm* of Shanghai Metro Line 1 qual to 4108·10^6 and 2618·10^6 CNY, respectively, which indicates that the underestimation rate of the calculated expected mean seismic loss *Lm* may be as high as 50%. Therefore, it is concluded that the selection of the appropriate fragility curves is of utmost importance for a reliable seismic loss assessment.

5. Summary and conclusions

This study examined the effects of salient parameters, such as the soil conditions, tunnel burial depth, tunnel construction quality, and aging phenomena of the lining, on the direct seismic losses of circular tunnels in alluvial deposits. A practical approach for probabilistic seismic loss

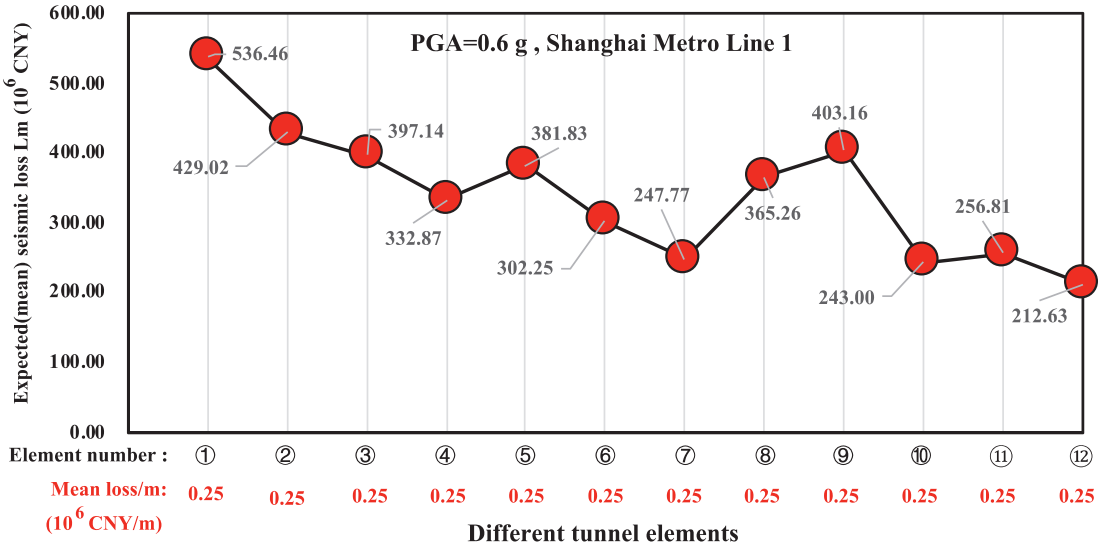

Fig. 15. Expected mean seismic loss *Lm* along 12 different tunnel elements of Shanghai Metro Line 1 at seismic intensity *PGA*= 0.6 g.

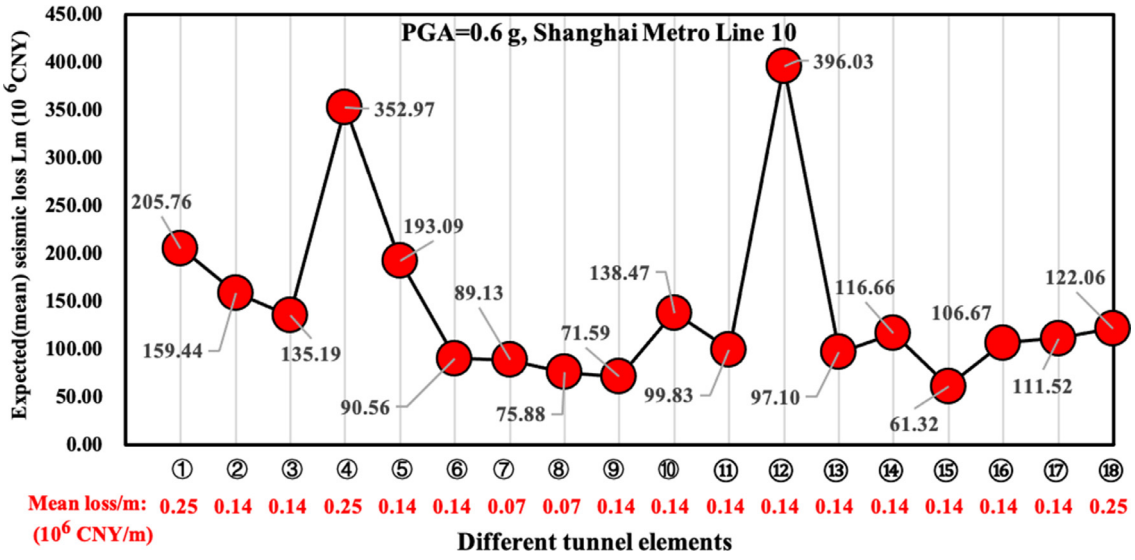

Fig. 16. Expected mean seismic loss *Lm* along 18 different tunnel elements of Shanghai Metro Line 10 at seismic intensity *PGA*= 0.6 g.

assessment of circular tunnels is proposed and employed, as an example, for this purpose on single tunnel segment in alluvial deposits, as well as on tunnel elements representative of the Shanghai Metro Lines 1 and 10, assuming various levels of selected seismic hazard.

Besides the general demonstration of the efficiency of the proposed methodology to probabilistic loss assessment of tunnel lines, like the ones in Shanghai, the following conclusions may be also drawn from the above analysis:

- The increase of the seismic hazard intensity leads, as expected, to more severe damage state of tunnel lining, ultimately increasing the expected mean seismic losses of the examined tunnel in alluvial deposits.
- For a given seismic hazard intensity, shallow tunnels with low construction quality embedded in softer soil conditions are generally associated with higher direct seismic losses compared to tunnels of better construction quality embedded in higher burial depths and stiffer soil conditions. To quantify the above general remark, it has been shown that for the examined tunnel segments, the differences in the calculated exceedance probability *Pl* of the tunnels due to different construction quality may be as high as 50%.
- It was demonstrated that the seismic structural losses of tunnels increase with an increase in the service years due to the effects of deterioration phenomena of the tunnel liners (corrosion) on the tunnel's vulnerability. It is important to notify that when applying this integrated approach the observed differences in the calculated exceedance probability *Pl* of the tunnels with different examined scenarios of service years may be as high as 59%.
- The above results are helpful for engineers to optimize the selection of the tunnel design parameters for different earthquake events and hazard levels. For instance, increasing the tunnel burial depth is generally an effective approach to mitigate the potential direct seismic loss of the tunnel. The outcome of this study will also improve prioritization for risk mitigation measures, and design appropriate recovery planning to enhance the seismic resilience of city infrastructure.

The present study aims at contributing toward an integrated seismic loss and risk management of tunnels based on the principles of infrastructure resilience. Nevertheless, some inevitable limitations of the study should be accounted for. Firstly, the tunnel direct cost assessment model, i.e., a mean loss ratio, is based on data from California, and it is

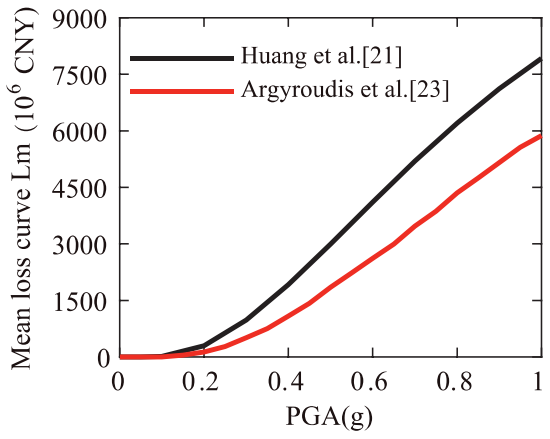

Fig. 17. Comparisons of expected mean seismic loss *Lm* of Shanghai Metro Line 1 using different fragility curves.

pretty simplified. There is a need to develop more rigorous tunnel direct cost assessment models, which will be able to consider more accurately the specific cost of tunnel construction and repairs along with associated uncertainties. Secondly, the indirect seismic losses, such as human casualties or indirect costs from additional travel time and distance due to tunnel closure, were not examined in this study, as this is a more complex process that involves social, technical, and economic factors [52–53]. Thirdly, the components, e.g., seismic hazard, fragility curves, loss ratios, and tunnel initial construction cost, in the proposed seismic loss assessment framework have a certain degree of uncertainty that has not been accounted for. Such uncertainties will be further considered and quantified in future research, assuming that they have a range of potential values or specific probability distributions. In this way, it is possible to present a range of values for the expected seismic losses. Fourthly, further research efforts are deemed to consider other factors affecting the seismic fragility of tunnels, e.g., rebar and bolt corrosion, water seepage, voids behind linings, and other forms of physical and chemical deterioration of the tunnel lining.

Declaration of Competing Interest

The authors declare that they have no known competing financial interests or personal relationships that could have appeared to influence the work reported in this paper.

CRediT authorship contribution statement

Zhongkai Huang: Conceptualization, Methodology, Formal analysis, Writing – original draft, Writing – review & editing, Data curation, Visualization. **Kyriazis Pitilakis:** Writing – review & editing, Methodology, Supervision. **Dongmei Zhang:** Funding acquisition, Project administration, Supervision. **Grigorios Tsinidis:** Writing – review & editing. **Sotirios Argyroudis:** Conceptualization, Methodology, Writing – review & editing, Supervision.

Acknowledgments

The first and third authors would like to thank the support of the National Natural Science Foundation of China (Grants No. 52108381, 51978517, 52090082), the National Key R&D Program (Grant No. 2021YFF0502200), and the China Postdoctoral Science Foundation (Grants No. 2022T150484, 2021M702491).

References

[1] Castillo JGS, Bruneau M, Elhami-Khorasani N. Seismic resilience of building inventory towards resilient cities. Resil Cities Struct 2022;1(1):1–12.
[2] Christopoulos C, Zhong C. Towards understanding, estimating and mitigating higher-mode effects for more resilient tall buildings. Resil Cities Struct 2022;1(1):53–64.
[3] Hashash YM, Hook JJ, Schmidt B, John I, Yao C. Seismic design and analysis of underground structures. Tunn Undergr Sp Technol 2001;16(4):247–93.
[4] Pitilakis K, Tsinidis G. Performance and seismic design of underground structures. In Earthquake geotechnical engineering design. Cham: Springer; 2014. p. 279–340.
[5] Tsinidis G, de Silva F, Anastasopoulos I, Bilotta E, Bobet A, Hashash YM, Fuentes R. Seismic behavior of tunnels: from experiments to analysis. Tunn Undergr Sp Technol 2020;99:103334.
[6] Iida H, Hiroto T, Yoshida N, Iwafuji M. Damage to Daikai subway station. Soils Found 1996;36(Special):283–300.
[7] Sayed MA, Kwon OS, Park D, Van NQ. Multi-platform soil-structure interaction simulation of Daikai subway tunnel during the 1995 Kobe earthquake. Soil Dyn Earthq Eng 2019;125:105643.
[8] Wang Z, Gao B, Jiang Y, Yuan S. Investigation and assessment on mountain tunnels and geotechnical damage after the Wenchuan earthquake. Sci China Ser E 2009;52(2):546–58.
[9] Yu H, Chen J, Bobet A, Yuan Y. Damage observation and assessment of the Longxi tunnel during the Wenchuan earthquake. Tunn Undergr Sp Technol 2016;54:102–16.
[10] Wang ZZ, Zhang Z. Seismic damage classification and risk assessment of mountain tunnels with a validation for the 2008 Wenchuan earthquake. Soil Dyn Earthq Eng 2013;45:45–55.
[11] Godschalk DR. Urban hazard mitigation: creating resilient cities. Nat Hazard Rev 2003;4(3):136–43.
[12] Chang SE, McDaniels T, Fox J, Dhariwal R, Longstaff H. Toward disaster-resilient cities: characterizing resilience of infrastructure systems with expert judgments. Risk Anal 2014;34(3):416–34.
[13] Saadat Y, Ayyub BM, Zhang Y, Zhang D, Huang H. Resilience of metrorail networks: quantification with Washington, DC as a case study. ASCE-ASME J Risk Uncertain Eng Syst B Mech Eng 2019;5(4):041011.
[14] Argyroudis SA, Mitoulis SA, Winter MG, Kaynia AM. Fragility of transport assets exposed to multiple hazards: state-of-the-art review toward infrastructural resilience. Reliab Eng Syst Saf 2019;191:106567.
[15] ALA (American Lifelines Alliance) Seismic Fragility Formulations for Water Systems: Guideline. Washington, DC: Federal Emergency Management Agency; 2001.
[16] Balkaya C, Kalkan E. Seismic vulnerability, behavior and design of tunnel form building structures. Eng Struct 2004;26:2081–99.
[17] Argyroudis S, Pitilakis K. Seismic fragility curves of shallow tunnels in alluvial deposits. Soil Dyn Earthq Eng 2012;35:1–12.
[18] Nguyen DD, Park D, Shamsher S, Nguyen VQ, Lee TH. Seismic vulnerability assessment of rectangular cut-and-cover subway tunnels. Tunn Undergr Sp Technol 2019;86:247–61.
[19] Zi H, Ding Z, Ji X, Liu Z, Shi C. Effect of voids on the seismic vulnerability of mountain tunnels. Soil Dyn Earthq Eng 2021;148:106833.
[20] Hu X, Zhou Z, Chen H, Ren Y. Seismic fragility analysis of tunnels with different buried depths in a soft soil. Sustainability 2020;12(3):892.
[21] Huang ZK, Pitilakis K, Tsinidis G, Argyroudis S, Zhang DM. Seismic vulnerability of circular tunnels in soft soil deposits: the case of Shanghai metropolitan system. Tunn Undergr Sp Technol 2020;98:103341.
[22] Huang ZK, Pitilakis K, Argyroudis S, Tsinidis G, Zhang DM. Selection of optimal intensity measures for fragility assessment of circular tunnels in soft soil deposits. Soil Dyn Earthq Eng 2021;145:106724.
[23] Argyroudis S, Tsinidis G, Gatti F, Pitilakis K. Effects of SSI and lining corrosion on the seismic vulnerability of shallow circular tunnels. Soil Dyn Earthq Eng 2017;98:244–56.
[24] Huang ZK, Argyroudis S, Zhang DM, Pitilakis K, Huang HW, Zhang DM. Time-dependent fragility functions for circular tunnels in soft soils. ASCE-ASME J Risk Uncertain Eng Syst 2022;8(3):04022030.
[25] He Z, Chen Q. Vertical seismic effect on the seismic fragility of large-space underground structures. Adv Civ Eng 2019;2019:9650294.
[26] He Z, Xu H, Gardoni P, Zhou Y, Wang Y, Zhao Z. Seismic demand and capacity models, and fragility estimates for underground structures considering spatially varying soil properties. Tunn Undergr Sp Technol 2022;119:104231.
[27] Tsinidis G, Karatzetzou A, Stefanidou S, Markogiannaki O. Developments in seismic vulnerability assessment of tunnels and underground structures. Geotechnics 2022;2(1):209–49.
[28] Baradaran SM, Yang TY, Elwood KJ. Seismic loss estimation of non-ductile reinforced concrete buildings. Earthq Eng Struct Dyn 2013;42(2):297–310.
[29] Gentile R, Galasso C. Simplified seismic loss assessment for optimal structural retrofit of RC buildings. Earthq Spectra 2021;37(1):346–65.
[30] Ghosh J, Padgett JE. Probabilistic seismic loss assessment of aging bridges using a component-level cost estimation approach. Earthq Eng Struct Dyn 2011;40(15):1743–61.
[31] Perdomo C, Monteiro R. Extension of displacement-based simplified procedures to the seismic loss assessment of multi-span RC bridges. Earthq Eng Struct Dyn 2021;50(4):1101–24.
[32] Fang C, Ping Y, Zheng Y, Chen Y. Probabilistic economic seismic loss estimation of steel braced frames incorporating emerging self-centering technologies. Eng Struct 2021;241:112486.
[33] Shirkhani A, Azar BF, Basim MC. Seismic loss assessment of steel structures equipped with rotational friction dampers subjected to intensifying dynamic excitations. Eng Struct 2021;238:112233.
[34] Pavel F, Vacareanu R. Seismic risk assessment for elements of the electric network in Romania. Buildings 2022;12(2):244.

[35] Shahnazaryan D, O'Reilly GJ, Monteiro R. On the seismic loss estimation of integrated performance-based designed buildings. Earthq Eng Struct Dyn 2022;51(8):1794–818.
[36] Selva J, Argyroudis S, Pitilakis K. Impact on loss/risk assessments of inter-model variability in vulnerability analysis. Nat Hazards 2013;67(2):723–46.
[37] Cartes P, Chamorro A, Echaveguren T. Seismic risk evaluation of highway tunnel groups. Nat Hazards 2021;108:2101–21.
[38] Cimellaro GP, Renschler C, Bruneau M. In Computational methods, seismic protection, hybrid testing and resilience in earthquake engineering. Cham: Springer; 2015. p. 151–83.
[39] Joyner MD, Gardner C, Puentes B, Sasani M. Resilience-Based seismic design of buildings through multi-objective optimization. Eng Struct 2021;246:113024.
[40] Shadabfar M, Mahsuli M, Zhang Y, Xue Y, Ayyub BM, Huang H, Medina RA. Resilience-based design of infrastructure: review of models, methodologies, and computational tools. ASCE-ASME J Risk Uncertain Eng Syst 2022;8(1):03121004.
[41] Abrahamson NA, Bommer JJ. Probability and uncertainty in seismic hazard analysis. Earthq Spectra 2005;21(2):603–7.
[42] Huang G, Qiu W, Zhang J. Modelling seismic fragility of a rock mountain tunnel based on support vector machine. Soil Dyn Earthq Eng 2017;102:160–71.
[43] Andreotti G, Lai CG. Use of fragility curves to assess the seismic vulnerability in the risk analysis of mountain tunnels. Tunn Undergr Sp Technol 2019;91:103008.
[44] Werner SD, Taylor CE, Cho S, Lavoie JP, Huyck C, Eitzel C, et al. REDARS 2: methodology and software for seismic risk analysis of highway systems (technical report, No. MCEER-06-SP08). Buffalo, NY: Multidisciplinary Center for Earthquake Engineering Research, State University of New York at Buffalo; 2006.
[45] Gazetas G, Gerolymos N, Anastasopoulos I. Response of three Athens metro underground structures in the 1999 Parnitha earthquake. Soil Dyn Earthq Eng 2005;25:617–33.
[46] Wang JY, Wang W, Cheng L. Discussion on reducing the construction cost of metro tunnels: taking Nanjing Metro as an example. Constr Econ 2004;7:37–40 in Chinese.
[47] CEN, EN 1998-1 Eurocode 8 design of structures for earthquake resistance. Brussels, Belgium: European Committee for Standardisation; 2004.
[48] Ma C, Lu D, Du X. Effect of buried depth on seismic response of rectangular underground structures considering the influence of ground loss. Soil Dyn Earthq Eng 2018;106:278–97.
[49] Sfahani MG, Guan H, Loo YC. Seismic reliability and risk assessment of structures based on fragility analysis—a review. Adv Struct Eng 2015;18(10):1653–69.
[50] Riga E, Karatzetzou A, Apostolaki S, Crowley H, Pitilakis K. Verification of seismic risk models using observed damages from past earthquake events. Bull Earthq Eng 2021;19(2):713–44.
[51] Silva V, Akkar S, Baker J, Bazzurro P, Castro JM, Crowley H, Vamvatsikos D. Current challenges and future trends in analytical fragility and vulnerability modeling. Earthq Spectra 2019;35(4):1927–52.
[52] Huang HW, Zhang DM, Huang ZK. Resilience of city underground infrastructure under multi-hazards impact: From structural level to network level. Resil Cities Struct 2022;1(2):76–86.
[53] Reis C, Lopes M, Baptista MA, Clain S. Towards an integrated framework for the risk assessment of coastal structures exposed to earthquake and tsunami hazards. Resil Cities Struct 2022;1(2):57–75.